

# Discrete Harmonic Functions from Local Coordinates

T. Bobach<sup>1</sup>, G. Farin<sup>2</sup>, D. Hansford<sup>2</sup>, G. Umlauf<sup>1</sup>

<sup>1</sup> CS Dept., University of Kaiserslautern  
{bobach|umlauf}@informatik.uni-kl.de

<sup>2</sup> School of Computing and Informatics, Prism Lab., Arizona State University  
{gerald.farin|dianne.hansford}@asu.edu

**Abstract.** In this work we focus on approximations of continuous harmonic functions by discrete harmonic functions based on the discrete Laplacian in a triangulation of a point set. We show how the choice of edge weights based on generalized barycentric coordinates influences the approximation quality of discrete harmonic functions. Furthermore, we consider a varying point set to demonstrate that generalized barycentric coordinates based on natural neighbors admit discrete harmonic functions that continuously depend on the point set.

## 1 Introduction

Harmonic functions are defined by a vanishing Laplacian and can be computed as the unique solution of the Laplace equation with given boundary conditions [1]. Discrete harmonic functions are defined in a broader, abstract sense on general graphs [2]. If the nodes of the graph are points in the plane and the edges arise from a triangulation, the discrete harmonic function is a discretization of its continuous counterpart. The discrete Laplacian, characterizing a discrete harmonic function, is now defined as a linear combination of the function values at a point and at its one-ring neighbors in the triangulation. Given a point set, both the triangulation and the coefficients (edge weights) in the linear combination can be chosen freely, thus influencing the quality of the discrete approximation of harmonic functions.

There exist many approaches to triangulate point sets, driven by as many different objectives [3]. For points that have no further attributes than their position in space, the Delaunay triangulation is a widely adopted method to produce an almost unique triangulation whose properties are beneficial in many applications.

The definition of edge weights in an effort to discretize the Laplacian has received considerable attention in the past. In surface mesh processing and finite element methods, cotangent coordinates, also known as discrete harmonic coordinates, are a well-known method, see e.g. [4, 5]. In the planar case, which is the focus of this paper, generalized barycentric coordinates of the points with respect to their one-ring neighborhood in the triangulation also provide good

approximations of the Laplacian. Generalized barycentric coordinates have been thoroughly studied for convex polygons [6], and have also been successfully derived for arbitrary polygons [7].

For point sets without explicit connectivity, the Voronoi diagram allows the definition of natural neighbor coordinates, which are generalized barycentric coordinates with various degrees of smoothness in an automatic neighborhood [8]. The duality of the Voronoi diagram and the Delaunay triangulation allows the comparison of natural neighbor coordinates to other generalized barycentric coordinates above. Three such natural neighbor coordinate methods are known as the  $C^0$ -smooth *Non-Sibsonian* coordinates [9–11],  $C^1$ -smooth *Sibson* coordinates [12], and  $C^2$ -smooth *Hiyoshi standard* coordinates [13].

*Overview:* We will start with the definition of discrete harmonic functions in Section 2, and revisit their computation in Section 3. In Section 4, we introduce six methods to compute generalized barycentric coordinates defined for polygons and arbitrary point sets in order to discretize the Laplacian. Section 5 compares discrete harmonic functions computed with the six discretizations in terms of approximation quality and suitability for spatially varying input data before concluding in Section 6.

## 2 Discrete Laplacian on Triangulations

A triangulation of a set of non-collinear points  $X = (\mathbf{x}_1, \dots, \mathbf{x}_n) \in \mathbf{R}^2$  is a partition of the convex hull  $\mathcal{C}(X)$  into triangles  $(\mathbf{x}_a, \mathbf{x}_b, \mathbf{x}_c)$  with edges  $e_{ab}, e_{bc}, e_{ca} \in E$ . The pair  $(X, E)$  is a directed, planar straight line graph with two directions on each non-boundary edge. The set of outgoing edges for a point  $\mathbf{x}_i$  defines its one-ring neighborhood  $N(\mathbf{x}_i) = \{\mathbf{x}_j | \exists e_{ij} \in E\}$ .

To minimize the arbitrariness in the choice of  $E$ , we choose the Delaunay triangulation  $\text{Del}(X)$  such that  $(X, E) = \text{Del}(X)$ . The circumcircle of a triangle in  $\text{Del}(X)$  does not contain any point from  $X$  in its interior, a property that uniquely and implicitly determines it up to ambiguous diagonals in the case of cocircular points [3].

Assume for now that we know weights  $\lambda_{ij} \in A$ ,  $\lambda_{ij} \geq 0$  for every edge  $e_{ij}$  and denote by  $G = (X, E, A)$  the directed, weighted graph represented by the triangulation. Then, we consider scalar-valued functions  $f_i := f(\mathbf{x}_i)$  on  $X$  and define the discrete Laplacian on  $G$ .

**Definition 1 (Discrete Laplacian  $\Delta$ ).** *On a connected, weighted graph  $G = (X, E, A)$  we define the discrete Laplacian of  $f$  at  $\mathbf{x}_i$  as*

$$\Delta f_i := \sum_{\mathbf{x}_j \in N(\mathbf{x}_i)} \lambda_{ij} (f_j - f_i). \quad (1)$$

The discrete Laplacian directly allows the definition of the local discrete harmonic property and discrete harmonic functions.

**Definition 2 (Harmonic at a Point; Pole).** Let  $G = (X, E, \Lambda)$  be a connected, weighted graph with  $\lambda_{ij} \geq 0$ . A function  $f : X \rightarrow \mathbf{R}$  is called harmonic at node  $\mathbf{x}_i$ , if

$$\Delta f_i = 0. \quad (2)$$

Otherwise  $f$  is said to have a pole at  $\mathbf{x}_i$ .

**Definition 3 (Discrete Harmonic Function).** Denote by  $P \subseteq X$  the set of poles for a function  $f : X \rightarrow \mathbf{R}$ , and by  $H = X \setminus P$  the set of nodes at which  $f$  is harmonic. Then,  $f$  is called a discrete harmonic function with poles  $P$  on  $G$ .

It is clear from the definition, that each non-constant discrete harmonic function has at least two poles, i.e. at its minimum and maximum, since the function cannot be harmonic there. The later use of generalized barycentric coordinates motivates the identification of  $H$  with interior points, which are contained in the convex hull of their neighborhood, and of  $P$  with boundary points,

$$H := \{\mathbf{x}_i | \mathbf{x}_i \in \mathcal{C}(N(\mathbf{x}_i))\}, \quad P := X \setminus H.$$

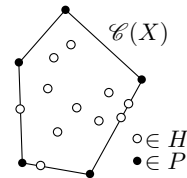


**Fig. 1.**

Note that there can be points in  $H \cap \partial \mathcal{C}(X)$ , see Figure 1. Finally, the following theorem ensures a unique solution for  $f$  based on given boundary conditions.

**Theorem 1.** Let  $G = (X, E, \Lambda)$  be a weighted, directed graph with  $\lambda_{ij} \geq 0$ . For every set  $P = X \setminus H$ , and every function  $f|_P : P \rightarrow \mathbf{R}$ , there is a unique function  $f|_H : H \rightarrow \mathbf{R}$  such that  $f|_X : X \rightarrow \mathbf{R}$  is a discrete harmonic function with poles  $P$  on  $G$ .

For a proof, see [14].

### 3 Discrete Harmonic Functions

Recall that continuous harmonic functions are the unique solution to the Laplace equation on a domain  $\Omega$  with boundary condition  $u$ ,

$$\Delta f = 0, \quad \text{s.t.} \quad f|_{\partial \Omega} = u.$$

Analogously,  $f|_H$  is the unique discrete harmonic extension of  $f|_P$  to  $f$  on  $G$ , i.e.  $f|_H$  is the solution to the discrete Laplace equation with boundary condition  $f|_P$ ,

$$\begin{aligned} \Delta f_i &= 0, & \text{for } v_i \in H, \\ \text{s.t.} \quad f_i &= u(v_i), & \text{for } v_i \in P. \end{aligned}$$

Using the abbreviation  $f_X = (f_H, f_P) \in \mathbf{R}^n$  for the column vector of  $f_i$  for all  $\mathbf{x}_i \in X$  and analogously  $f_H \in \mathbf{R}^m$ ,  $f_P \in \mathbf{R}^{(n-m)}$ , the Laplace operator  $\Delta f_H$  can be written, with appropriate reordering of  $X$ , as

$$\Delta f_H = f_H - S f_X = [(\mathbf{I} - S^H) \quad S^P] \begin{bmatrix} f_H \\ f_P \end{bmatrix} = (\mathbf{I} - S^H) f_H + S^P f_P,$$

where  $S \in \mathbf{R}^{m \times n}$  with  $S_{ij} = \lambda_{ij}$  if  $v_i \in H$  and  $v_j \in V$ , and  $S_{ij} = 0$  otherwise, and  $S = [S^H \ S^P]$  is the partition into  $S^H \in \mathbf{R}^{m \times m}$  and  $S^P \in \mathbf{R}^{m \times (n-m)}$ . Setting  $\Delta f_H = 0$  and solving for  $f_H$  yields

$$f_H = \underbrace{(\mathbf{I} - S^H)^{-1} S^P}_{=: M} f_P.$$

We see that  $M$  is only defined if  $(\mathbf{I} - S^H)$  is invertible, which follows directly from Theorem 1 for positive weights.

*Remark 1.* The existence of  $M$  is also guaranteed by  $\mathbf{I} - S^H$  being weakly diagonally dominant and irreducible. See [15] for a proof.

## 4 Local Coordinates

We have defined  $\text{Del}(X)$  and presented the computation of the discrete harmonic function  $f_H$  from  $f_P$  under the assumption that  $\lambda_{ij} \geq 0$  are known. We now turn our attention to the computation of  $\lambda_{ij}$  from generalized barycentric coordinates.

By definition,  $\mathbf{x}_i \in H$  can be expressed as a convex combination of  $N(\mathbf{x}_i)$ ,

$$\mathbf{x}_i = \sum_{\mathbf{x}_j \in N(\mathbf{x}_i)} \lambda_{ij} \mathbf{x}_j, \quad \sum_{\mathbf{x}_j \in N(\mathbf{x}_i)} \lambda_{ij} = 1, \quad \lambda_{ij} \geq 0. \quad (3)$$

For  $\mathbf{x}_i \in P$ , there are in general no  $\lambda_{ij}$  with the above property. Since we do not need  $\Delta_i, \mathbf{x}_i \in P$ , we ignore them.

Obviously, property (2) of discrete harmonic functions directly corresponds to the *local coordinate property* (3), which we can rewrite as

$$0 = \Delta \mathbf{x}_i = \sum_{\mathbf{x}_j \in N(\mathbf{x}_i)} \lambda_{ij} (\mathbf{x}_j - \mathbf{x}_i), \quad \mathbf{x}_i \in H. \quad (4)$$

Thus, the coordinate functions of  $\mathbf{x}_i$  are harmonic functions on  $G$  with poles in  $P$ . The local coordinates  $\lambda_{ij}$  are coefficients in (4). If the positions in  $X$  change, their smoothness with respect to the positions in  $X$  governs the smoothness of the discrete Laplacian.

For  $|N(\mathbf{x}_i)| > 3$ , the  $\lambda_{ij}$  are not unique. We discuss the choice of local coordinates in the sequel.

### 4.1 Generalized Barycentric Coordinates in Polygons

In  $\text{Del}(X)$ , each point  $\mathbf{x}_i \in H$  is contained in the kernel of the simple polygon formed by the points of the oriented neighborhood  $N(\mathbf{x}_i)$ , which allows the computation of a wide spectrum of well-understood polygonal barycentric coordinates for  $\mathbf{x}_i$ . We consider cotangent- [5], Wachspress- [16], and mean value coordinates [17], which we refer to by  $A^c$ ,  $A^w$ , and  $A^m$ , respectively. Note that Wachspress coordinates become negative in non-convex polygons.<sup>1</sup>

<sup>1</sup> In all our test cases,  $M$  was well defined.

The above are rational functions of the vertices of the enclosing polygon with linear precision on its edges. Polygonal barycentric coordinates smoothly depend on the vertices of the enclosing polygon, but in general do not agree if the enclosing polygon changes. This observation is important if the positions in  $X$  vary, as the neighborhood in  $\text{Del}(X)$  may change with  $X$ .

We now give the definition of the barycentric coordinates used in our assessment.

**Definition 4 (Cotangent coordinates [5]).** Let  $\beta_{ij}$ , and  $\gamma_{ij}$  denote the angles as shown in Figure 2. Then,

$$\lambda_{ij}^c := \frac{\tilde{\lambda}_{ij}^c}{\sum_{\mathbf{x}_k \in N(\mathbf{x}_i)} \tilde{\lambda}_{ik}^c}, \quad \tilde{\lambda}_{ij}^c = \cot(\beta_{ij-1}) + \cot(\gamma_{ij})$$

is called cotangent coordinate of  $\mathbf{x}_i$  with respect to  $\mathbf{x}_j$ .

**Definition 5 (Wachspress coordinates [16]).** Let  $\beta_{ij}$ , and  $\gamma_{ij}$  denote the angles as shown in Figure 2. Then,

$$\lambda_{ij}^w = \frac{\tilde{\lambda}_{ij}^w}{\sum_{\mathbf{x}_k \in N(\mathbf{x}_i)} \tilde{\lambda}_{ik}^w}, \quad \tilde{\lambda}_{ij}^w = \frac{\cot(\beta_{ij}) + \cot(\gamma_{ij-1})}{\|\mathbf{x}_i - \mathbf{x}_j\|^2}$$

is called Wachspress coordinate of  $\mathbf{x}_i$  with respect to  $\mathbf{x}_j$ .

**Definition 6 (Mean value coordinates [17]).** Let  $\alpha_{ij}$ , denote the angles as shown in Figure 2. Then,

$$\lambda_{ij}^m = \frac{\tilde{\lambda}_{ij}^m}{\sum_{\mathbf{x}_k \in N(\mathbf{x}_i)} \tilde{\lambda}_{ik}^m}, \quad \tilde{\lambda}_{ij}^m = \frac{\tan(\alpha_{ij-1}/2) + \tan(\alpha_{ij}/2)}{\|\mathbf{x}_i - \mathbf{x}_j\|}$$

is called mean value coordinate of  $\mathbf{x}_i$  with respect to  $\mathbf{x}_j$ .

## 4.2 Natural Neighbor Coordinates

Natural neighbor coordinates are generalized barycentric coordinates which are defined independent of any explicit adjacency on  $X$ , based on the implicit adjacency defined by the Voronoi diagram. However, the Delaunay triangulation is dual to the Voronoi diagram, and the set  $N(\mathbf{x}_i)$  coincides with the set of natural neighbors upon which the coordinates are defined.

Three methods for the computation of natural neighbor coordinates are known as Non-Sibsonian- [10], Sibson- [12], and Hiyoshi standard natural neighbor coordinates [13], which we refer to by  $A^n$ ,  $A^s$ , and  $A^h$ , respectively. They mainly differ in their smoothness with respect to  $\mathbf{x}_i$ .

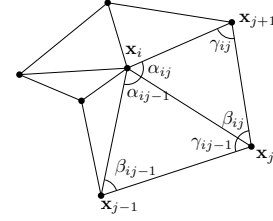


**Fig. 2.** Angles used in computations.

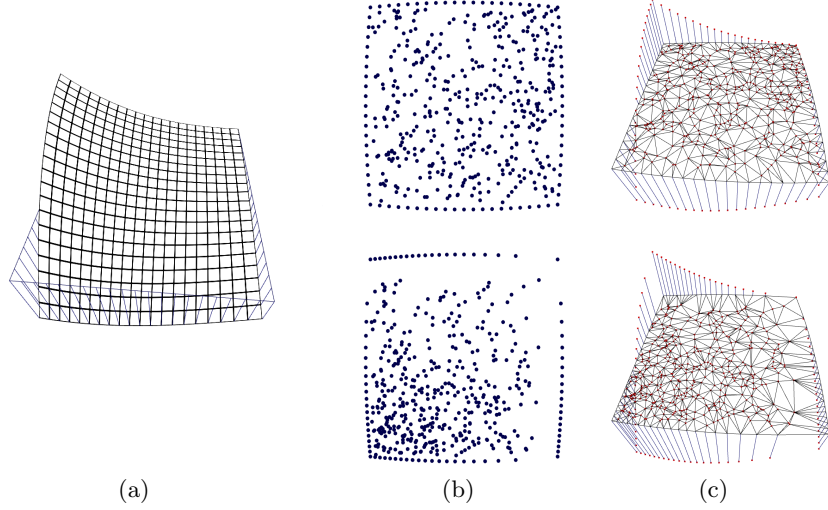


**Fig. 3.** Homogeneous (upper row) and inhomogeneous (lower row) setting. (a) Graph of the function  $g(x, y) = \frac{1}{3}x^3 - xy^2$ , (b) point distribution, (c) Delaunay triangulation and values at the boundary.

Before defining natural neighbor coordinates, we need to introduce the Voronoi diagram  $\text{Vor}(X)$  as the dual of  $\text{Del}(X)$  in the sense that each edge  $e_{ij}^{\text{Vor}}$  is dual to  $e_{ij}$  and connects the circumcenters of two adjacent triangles. The polygon formed by the circumcenters of the Delaunay triangles adjacent to  $\mathbf{x}_i$  is called its *Voronoi tile*  $\mathcal{T}_i$ .

**Definition 7 (Non-Sibsonian coordinates [10]).** Let  $\|e_{ij}\|$  and  $\|e_{ij}^{\text{Vor}}\|$  denote the lengths of  $e_{ij}$  and its dual  $e_{ij}^{\text{Vor}}$ , then

$$\lambda_{ij}^n = \tilde{\lambda}_{ij}^n / \left( \sum_{\mathbf{x}_k \in N(\mathbf{x}_i)} \tilde{\lambda}_{ik}^n \right), \quad \tilde{\lambda}_{ij}^n = \|e_{ij}^{\text{Vor}}\| / \|e_{ij}\|$$

is called Non-Sibsonian coordinate of  $\mathbf{x}_i$  with respect to  $\mathbf{x}_j$ .

*Remark 2.* Note that, given the same set of neighbors, cotangent coordinates are by construction identical to Non-Sibsonian coordinates, which is shown in [18]. Consequently, cotangent coordinates on Delaunay triangulations belong to the family of natural neighbor coordinates.

**Definition 8 (Sibson coordinates [12]).** Let  $X = (\mathbf{x}_1, \dots, \mathbf{x}_n) \in \mathbf{R}^2$ , and  $X^{(i)} := X \setminus \{\mathbf{x}_i\}$ . Let  $\mathcal{T}_i$  be the Voronoi tile of  $\mathbf{x}_i$  in  $\text{Vor}(X)$ , and  $\{\mathcal{T}_j^{(i)}\}_{\mathbf{x}_j \in N(\mathbf{x}_i)}$  the Voronoi tiles of its neighbors in  $\text{Vor}(X^{(i)})$ . Then, with  $|\cdot|$  denoting the area in  $\mathbf{R}^2$ ,

$$\lambda_{ij}^s = |\mathcal{T}_i \cap \mathcal{T}_j^{(i)}| / |\mathcal{T}_i|$$

is called Sibson coordinate of  $\mathbf{x}_i$  with respect to  $\mathbf{x}_j$ .

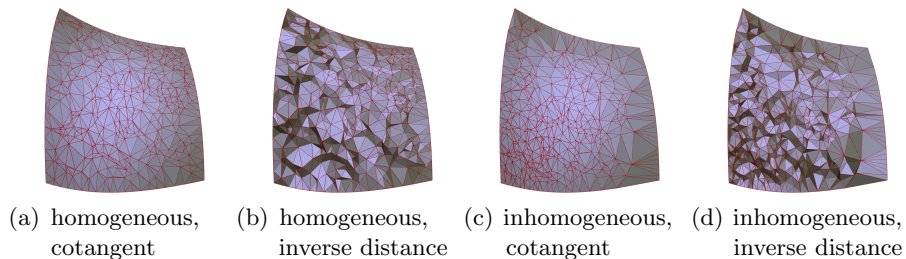


**Fig. 4.** Delaunay triangulation of  $X$  in 2.5D, the  $z$ -axis representing the values of  $f_i$  for the solution based on cotangent coordinates in (a),(c), and the solution based on inverse distance weights in (b),(d).

Hiyoshi standard coordinates emerge from a relationship by which one can express  $\lambda_{ij}^s$  as an integral over  $\lambda_{ij}^n$  in the context of power diagrams. The repeated application of this integral relation leads to a whole family of local coordinates with increasing order of smoothness. Because a complete definition of Hiyoshi standard coordinates does not fit the scope of this paper, we refer the reader to [13] and denote Hiyoshi  $C^2$  (standard) coordinates by  $\lambda_{ij}^h$ .

*Remark 3.* In  $X$ ,  $\lambda_{ij}^n$  are continuous,  $\lambda_{ij}^s$  are  $C^1$ -smooth, and  $\lambda_{ij}^h$  are  $C^2$ -smooth with respect to  $\mathbf{x}_i$ . Although the definitions above are not directly applicable for  $\mathbf{x}_i \in H \cap \mathcal{C}(X)$ , they can be extended accordingly by a limit argument. For  $\mathbf{x}_i \in P$ , this is not possible and  $\lambda_{ij}^l$ ,  $\lambda_{ij}^s$ ,  $\lambda_{ij}^h$  are not defined.

## 5 Comparison

In this section, we first discuss the experimental approximation quality of discrete harmonic functions based on one of the Laplacian discretizations presented in Section 4. Then, we illustrate the difference between generalized barycentric coordinates on polygons and natural neighbor coordinates in Laplacian discretizations on point sets with variable positions.

### 5.1 Experimental Approximation Quality

We now compare discrete harmonic functions computed using the Laplacian discretizations based on coordinates from Section 4 by considering function values sampled from the harmonic function

$$g(x, y) = \frac{1}{3}x^3 - xy^2$$

over the domain  $\Omega = [0.3, 1.3] \times [0.1, 1.1]$  to compute approximate solutions  $f^\bullet$ ,  $\bullet \in \{c, w, m, n, s, h\}$  to the Laplace equation with boundary conditions sampled from  $g$ . The graph of  $g$  is depicted in Figure 3(a). To illustrate the effect of a

Coordinates used for approximation	Homogeneous point distribution		Inhomogeneous point distribution	
	RMS	MAX	RMS	MAX
Non-Sibsonian coordinates	7.08e-8	1.08e-3	3.22e-7	3.88e-3
Sibson coordinates	2.53e-6	3.65e-3	1.92e-6	4.20e-3
Hiyoshi coordinates	5.78e-6	5.44e-3	3.57e-6	4.66e-3
Cotangent coordinates	7.08e-8	1.08e-3	3.22e-7	3.88e-3
Mean value coordinates	5.60e-6	4.85e-3	7.37e-6	7.04e-3
Wachspress coordinates	2.53e-5	1.10e-2	2.09e-5	1.18e-2
Inverse distance weights	5.43e-4	9.32e-2	8.76e-4	8.09e-2

**Table 1.** Comparison of root mean square (RMS) error and maximum absolute deviation (MAX) for the per-point error  $|f(\mathbf{x}_i) - g(\mathbf{x}_i)|$ .

Laplacian discretization that does not arise from barycentric coordinates but still tries to capture the spatial relation between the nodes, our comparison includes inverse distance weights,

$$\lambda_{ij}^{id} := \|\mathbf{x}_i - \mathbf{x}_j\|^{-1} / \sum_{\mathbf{x}_k \in N(\mathbf{x}_i)} \|\mathbf{x}_i - \mathbf{x}_k\|^{-1}.$$

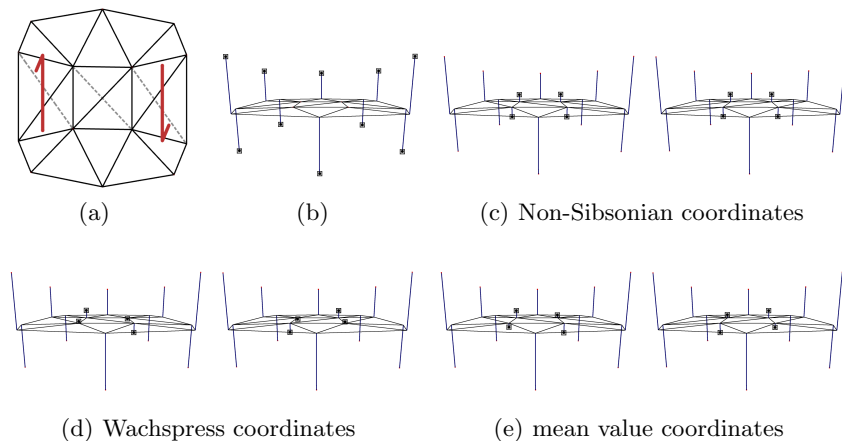
We choose two distributions of  $|X| = 480$  points in  $\Omega$ : homogeneous as in Figure 3(b), top row, and inhomogeneous as in Figure 3(b), bottom row, which helps examine the influence of how well the domain is covered by sample points. In Figure 3(c) the Delaunay triangulation and the imposed boundary conditions are shown.

Table 1 shows the analysis of the per-point errors and indicates that Non-Sibsonian- and cotangent coordinates yield the lowest error, while the others are worse by orders of magnitude. Furthermore, it seems that this discrepancy is less prominent in the inhomogeneous setting for natural neighbor coordinates.

Figure 4 shows the visual comparison of  $f^c$  and  $f^{id}$ . The results obtained using any of the local coordinates in the Laplacian discretization are visually indistinguishable from the exact solution sampled from  $g$  (Figure 4(a) and (c)). As Figure 4(b) and (d) show, there are considerable distortions if the coordinate functions are not harmonic as with  $\Lambda^{id}$ .

## 5.2 Varying Positions

We are now interested in how discrete harmonic functions based on the different Laplacian discretizations behave if the positions of the point set vary. Figure 5(a) shows  $\text{Del}(X)$  for a simple setting with  $|H| = 4$ ,  $|P| = 10$ , which we deliberately choose to contain three sets of cocircular points. We assume the origin in the center of the dataset and shear the points in the direction indicated by the arrows, thus causing the ambiguous diagonals to flip between two possible positions as indicated by the dashed lines. Note that such flips occur in any



**Fig. 5.** (a) With the origin at the center of the data set and shear in the direction indicated by the arrows, the ambiguous Delaunay triangulation flips between two possible diagonal directions, depicted by the dashed lines. (b) The thick dots denote the values imposed as boundary condition, the interior four vertices are to be computed. (c)-(e) The thick dots indicate the computed discrete harmonic function values at the vertices of the triangulation. The left and right pictures show the values for the two different diagonal directions. Note the jumps in (d), (e) which does not occur in (c).

triangulation if the deformation of the point set is big enough. Because the alternating boundary values shown in Figure 5(b) are horizontally symmetric, the discrete harmonic function should be, too.

Figure 5 shows the results of computing the discrete harmonic function on the point set under a shearing deformation, just before and after the diagonal flip. The results for cotangent, Non-Sibsonian, Sibson, and Hiyoshi standard coordinates are visually indistinguishable, which is why we only show one representative picture in Figure 5(c). First, notice how both Wachspress in Figure 5(d) and mean value coordinates in Figure 5(e) result in an asymmetric harmonic function in spite of the symmetry in the point set and the values. As long as the triangulation stays the same, the harmonic function for all approaches continuously follows the deformation. As a result of the diagonal flip, however, the polygonal coordinates show a discontinuous change in the harmonic function, which is not the case for natural neighbor coordinates.

## 6 Conclusion

In this paper, we have compared different discretizations of the Laplacian, applied to the computation of discrete harmonic functions from prescribed boundary values. To this end, we used the Delaunay triangulation and generalized barycentric coordinates in the Delaunay neighborhoods and focused on two classes of coordinates, defined on polygons and on natural neighbors.

First, we assessed the approximation quality by sampling the boundary values from a known harmonic function and comparing it to the computed discrete harmonic function. Although all approaches based on generalized barycentric coordinates provide acceptable results, we found that those based on Non-Sibsonian-coordinates, which are in our setting identical to cotangent coordinates, have the lowest approximation error and that by several orders of magnitude.

Second, we used a point set with fix boundary values but variable positions to analyze the effect of triangulation changes on the discrete harmonic function. We have showed that except for cotangent coordinates, those based on polygons yield discontinuous changes in the harmonic function under modifications in the triangulation. The reason for cotangent coordinates to behave differently lies in their equality to Non-Sibsonian coordinates if computed on a Delaunay triangulation, thus effectively representing natural neighbor coordinates. The latter always admit harmonic functions that continuously change with the positions of the point set, making them especially suited for application on variable point sets.

We are positive that within an appropriate framework these results also apply to the manifold case. One promising method is that of [19] which provides a setting similar to the one we used in this paper on manifolds.

## Acknowledgments

This work was supported by the international graduate school DFG grant 1131 on “Visualization of Large and Unstructured Data Sets - Applications in Geospatial Planning, Modeling and Engineering”. Farin and Hansford were supported by an NSF grant 0306385 “Splines over Iterated Voronoi Diagrams”.

## References

1. Axler, S., Bourdon, P., Ramey, W.: Harmonic Function Theory. 2nd edn. Springer (2001)
2. Benjamini, I., Lovász, L.: Harmonic and analytic functions on graphs. *J. of Geometry* **76** (2003) 3–15
3. Hjelle, Ø., Dæhlen, M.: Triangulations and Applications. Mathematics and Visualization. Springer, Secaucus, NJ, USA (2006)
4. Eck, M., DeRose, T., Duchamp, T., Hoppe, H., Lounsbery, M., Stuetzle, W.: Multiresolution analysis of arbitrary meshes. *Computer Graphics* **29**(Annual Conference Series) (1995) 173–182
5. Iserles, A.: A First Course in Numerical Analysis of Differential Equations. Cambridge University Press (1996)
6. Warren, J., Schaefer, S., Hirani, A.N., Desbrun, M.: Barycentric coordinates for convex sets. *Advances in Computational Mathematics* (2005) to appear
7. Hormann, K.: Barycentric coordinates for arbitrary polygons in the plane. Technical Report IfI-05-05, Department of Informatics, Clausthal University of Technology (Feb 2005)

8. Bobach, T., Umlauf, G.: Natural neighbor interpolation and order of continuity. In: *GI Lecture Notes in Informatics: Visualization of Large and Unstructured Data Sets*, Springer (2006) 69–86
9. Christ, N.H., Friedberg, R., Lee, T.D.: Weights of links and plaquettes in a random lattice. *Nuclear Physics B* **210(3)** (1982) 337–346
10. Belikov, V., Ivanov, V., Kontorovich, V., Korytnik, S., Semenov, A.: The non-Sibsonian interpolation: A new method of interpolation of the values of a function on an arbitrary set of points. *Comp. Mathematics and Mathematical Physics* **37(1)** (1997) 9–15
11. Sugihara, K.: Surface interpolation based on new local coordinates. *Computer Aided Design* **13(1)** (1999) 51–58
12. Sibson, R.: A vector identity for the Dirichlet tessellation. *Math. Proc. of Cambridge Philosophical Society* **87** (1980) 151–155
13. Hiyoshi, H., Sugihara, K.: Voronoi-based interpolation with higher continuity. In: *Symposium on Comp. Geom.* (2000) 242–250
14. Lovász, L.: Discrete analytic functions: a survey. Technical report, Microsoft Research (2000)
15. Varga, R.S.: *Matrix Iterative Analysis*. PrenticeHall, Englewood Cliffs, NJ, USA (1962)
16. Wachspress, E.: *A rational finite element basis* (1975) Academic Press.
17. Floater, M.S.: Mean value coordinates. *Comput. Aided Geom. Des.* **20(1)** (2003) 19–27
18. Ju, T., Liepa, P., Warren, J.: A general geometric construction of coordinates in a convex simplicial polytope. *Computer Aided Geometric Design* **24** (April 2007) 161–178
19. Flötotto, J.: A coordinate system associated to a point cloud issued from a manifold: definition, properties and applications. PhD thesis, Université de Nice-Sophia Antipolis (Sep 2003) <http://www.inria.fr/rrrt/tu-0805.html>.